Journal of Dental Research
DS1–DS4

DOI: 10.1177/0022034515625939
jdr.sagepub.com

Evidence for Bicarbonate Secretion by Ameloblasts in a Novel Cellular Model

E. Bori[1], J. Guo[2], R. Rácz[1], B. Burghardt[1], A. Földes[1], B. Kerémi[1], H. Harada[3], M.C. Steward[4], P. Den Besten[5], A.L.J.J. Bronckers[2], and G. Varga[1]

Appendix

Materials and Methods

Measurement of transepithelial electrical resistance. HAT-7 cells grown on Transwells were incubated in 12-well plates. Transepithelial electrical resistance (TER) values were measured with an epithelial voltohmmeter (World Precision Instruments, Hamden, CT, USA) on 7 consecutive days to characterize the time course of tight junction formation. Once confluence has been reached, the TER values also give an indication of the paracellular permeability to electrolytes, an important characteristic of secretory and absorptive epithelia. TER was measured routinely before each functional measurement and before fixation for immunohistochemistry.

Immunohistochemistry. HAT-7 cells cultured on Transwells were fixed in 4% buffered paraformaldehyde, with the filters removed from the plastic inserts and cut into strips. Some strips were processed for paraffin cross sections, dewaxed, and immunoreacted with primary rabbit antibodies, followed by incubation with a peroxidase-conjugated goat anti-rabbit secondary antibody (Envision Kit, DakoPatt, Copenhagen, Denmark). The peroxidase was developed with DAB and the sections counterstained with hematoxylin. To obtain an en face view, other strips were transferred to 48-well plates, rinsed in phosphate-buffered saline containing Triton X-100 (0.2% v/v), immunoreacted with primary antibodies, and followed by incubation with either goat anti-rabbit conjugated with Alexa-488 (1:200; Invitrogen, Franklin Lakes, NY, USA) or goat anti-rabbit with peroxidase (1:500; Thermo Scientific, Waltham, MA, USA). In cells immunostained with Alexa 488 fluorescent labels, the nuclei were counterstained with propidium iodine (1 µg/mL), mounted on glass slides in Vectashield mounting medium (Vector Laboratories, Peterborough, UK), and covered with a glass coverslip. Micrographs of the filters were taken with a Leica microscope with transmitted light. The following primary antibodies were used: rabbit anti-zonula occludens-1 (1:200; Zymed Laboratories, San Francisco, CA, USA), rabbit anti-KLK4 (1:200, purified on protein G minicolumns; donated by Dr. J. Simmer, MI, USA), affinity-purified rabbit anti-amelotin (1:100 to 1:200; courtesy of Dr. B. Ganss, Toronto, Canada) or normal nonimmune rabbit IgG as negative control (DakoPatt), rabbit anti-carbonic anhydrase-II (1:800 to 1:1000, catalog SC 25596; Santa Cruz Biotechnology, Dallas, TX, USA; Reibring et al. 2014), rabbit anti-NBCe1 serum (1:600, purified on a protein G minicolumn; a gift from Dr. W. Boron, Cleveland, OH, USA; Jalali et al. 2014), affinity-purified rabbit anti-AE2 (1:50 to 1:100; a gift from Dr. S. Kellokumpu, Oulu, Finland; Bronckers et al. 2009), rabbit anti-pendrin (1:100; Santa Cruz Biotechnology; Bronckers et al. 2011), and rabbit anti-CFTR (1:200; Alomone Labs, Jerusalem, Israel). Rabbit antibody to Slc26a6 was kindly provided by Dr P. Aronson (Yale University, New Haven, CT, USA) and its specificity validated on Slc26a6-null ameloblasts (Jalali et al. 2015). Except for NBCe1, all other antibodies required antigen retrieval in hot 10mM citrate buffer (pH 6.0) for 20 min. Anti-NBCe1, anti-AE2, and anti-pendrin were previously validated by testing on null mouse tissue.

RT-PCR and RT-qPCR. The expression of tight junction proteins, transporters, and ameloblast markers was investigated at the RNA level by RT-PCR (reverse transcription polymerase chain reaction). We also tested these proteins by RT-qPCR (real-time quantitative polymerase chain reaction). RNA was isolated 4 d after seeding from parallel plastic, control, differentiation, and hepato-STIM samples by Nucleospin RNA II kit (Macherey-Nagel, Düren, Germany) and from rat organs that were used as positive control by TRI reagent (Sigma-Aldrich, St. Louis, MO, USA). Approximately 1 to 2 µg of total RNA was reverse transcribed by Maxima First Strand cDNA Synthesis Kit for RT-qPCR (Thermo Scientific). The cDNA was then used in conventional and/or quantitative PCR (polymerase chain reaction). In conventional PCR, self-designed primers and Maxima

[1]Department of Oral Biology, Semmelweis University, Budapest, Hungary
[2]Department of Oral Cell Biology, Academic Centre for Dentistry Amsterdam, University of Amsterdam and VU University Amsterdam, MOVE Research Institute, Amsterdam, Netherlands
[3]Department of Anatomy, Division of Developmental Biology and Regenerative Medicine, Iwate Medical University, Iwate, Japan
[4]Faculty of Life Sciences, The University of Manchester, Manchester, UK
[5]Department of Orofacial Sciences, University of California, San Francisco, CA, USA

Corresponding Author:
G. Varga, H-1089 Budapest, Nagyvárad tér 4, Hungary.
Email: varga.gabor@dent.semmelweis-univ.hu

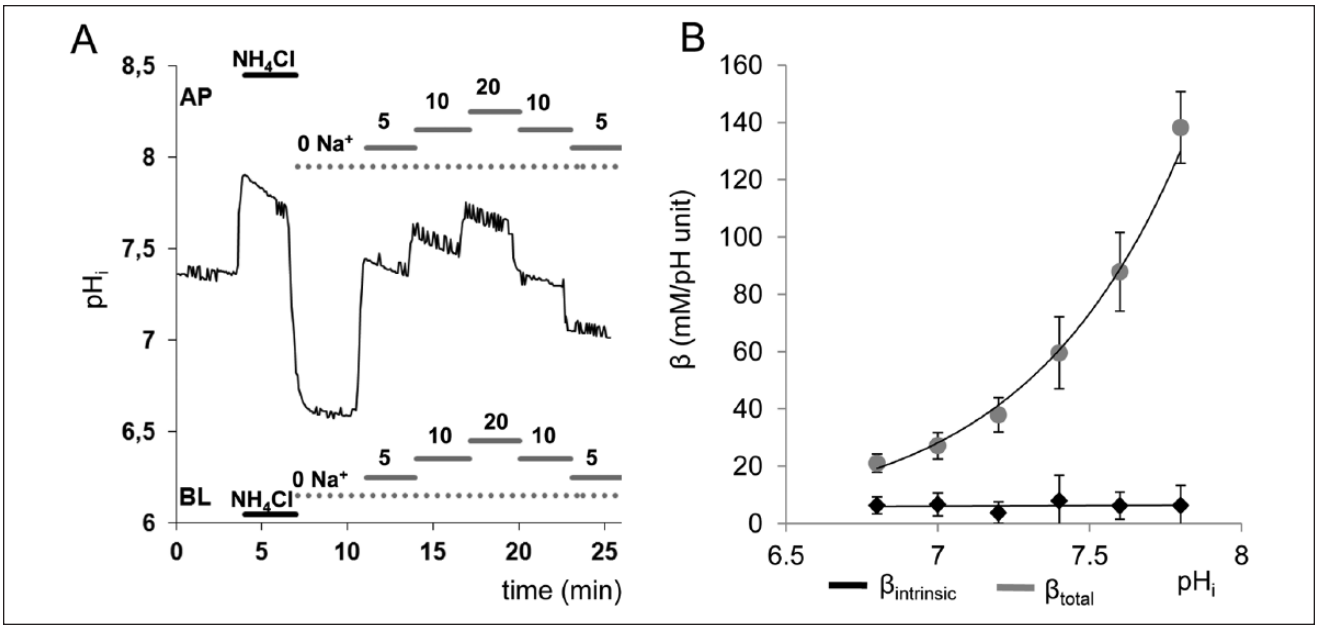

Appendix Figure. Buffering capacity of HAT-7 cells. Intrinsic buffering capacity was evaluated by measuring intracellular pH (pH_i) during a stepwise increase and decrease in NH_4^+ concentration (5, 10, and 20 mM) in the absence of extracellular Na^+. (**A**) A typical intrinsic buffering capacity measurement. (**B**) Total buffering capacity ($ß_{total}$, gray) and intrinsic buffering capacity ($ß_{intrinsic}$, black) plotted against intracellular pH. Data represent mean ± SEM (n = 6). A trend line was fitted by nonlinear regression to the $ß_{total}$ data and used to determine values for the calculation of base fluxes. AP, apical perfusate; BL, basolateral perfusate.

Hot Start Green PCR Master Mix (Thermo Scientific) were used. Primer details and reaction conditions are given in Appendix Table 1. In conventional PCR, β-actin was used as internal control. PCR products were electrophoresed in 1.8% TAE agarose (VWR International, Radnor, PA, USA) and compared with a GeneRuler 100 bp DNA Ladder (Thermo Scientific). PCR products were sequenced with the original samples, depicted in Figure 2 of main text. BLAST analyses revealed 95% to 99% identity with the concensus sequence in each case. Also, these analyses showed that no other known gene sequences were identical or greatly similar to the sequenced PCR products.

RT-qPCR amplification was performed with the ABI StepOne System with TaqMan Universal Master Mix II and predesigned primers (Appendix Table 2; Applied Biosystems, Foster City, CA, USA). Acidic ribosomal protein P0 (Rplpo) was used as internal control (Szlavik et al. 2008), and the ΔΔCt method was used to quantify gene expression.

Microfluorometry. Bicarbonate transport in HAT-7 cells was measured by microfluorometry as described previously (Szucs et al. 2006). Briefly, the cells were loaded with a fluorescent dye, BCECF, that is sensitive to intracellular pH (pH_i) and therefore capable of indirectly measuring H^+ and/or HCO_3^- movements through the cell membrane. By controlling the extracellular environment (e.g., specific ion withdrawal, application of transporter inhibitors), particular elements of HCO_3^- transport can be identified. The so-called ammonium pulse technique was applied when an acid load was necessary to examine the transporters involved in compensation of these pH changes. At the end of the measurements, the cells were treated with 0.5% Triton X-100 to release the BCECF and determine the autofluorescence.

The Transwell samples were mounted in a purpose-built chamber on a Nikon Eclipse TE200 inverted fluorescence microscope and were perfused bilaterally at 3 mL/min. Fluorescence was measured at 530 nm every 5 s with a photomultiplier tube and amplifier (Cairn Research, Faversham, Kent, UK), and data were acquired with DASYLab Software (Measurement Computing, Norton, MA, USA). Illumination was alternated between 490- and 440-nm excitation wave lengths, and the fluorescence data were corrected for autofluorescence. The ratio of fluorescence signals at the 2 excitation wave lengths was converted to pH with calibration data obtained through the nigericin/high potassium method (Thomas et al. 1979).

Solutions and pharmacologic agents used for microfluorometry. The following solutions were used for perfusion: standard HEPES-buffered solution containing 137mM NaCl, 5mM KCl, 1mM $CaCl_2$, 1mM $MgCl_2$, 10mM D-glucose, and 10mM HEPES, equilibrated with 100% O_2; standard HCO_3^--buffered solution containing 116mM NaCl, 25mM $NaHCO_3$, 5mM KCl, 1mM $CaCl_2$, 1mM $MgCl_2$, 10mM D-glucose, and 5mM HEPES, equilibrated with 5% CO_2 / 95% O_2. For Na^+ withdrawal, Na^+ was replaced by equimolar N-methyl-D-glucamine ($NMDG^+$), and for NH_4Cl addition, the amount of NaCl/NMDG-Cl was reduced to ensure iso-osmolality. All solutions were adjusted to pH 7.4 at 37 °C. For inhibiting specific transport processes, 300μM amiloride or 10μM cariporide was used

Appendix Table 1. Primers.

Name	Forward Primer	Reverse Primer	Product Length, bp	Annealing Temperature, °C
Actb	5′-CCCTGAAGTACCCCATTGAA-3′	5′-CCCTCATAGATGGGCACAGT-3′	307	55
Tjp1	5′-CAAAGAGATGAGCGGGCTAC-3′	5′-AAATCCACATCTGGCTGTCC-3′	416	50
Cldn1	5′-AGGTCTGGCGACATTAGTGG-3′	5′-CGTGGTGTTGGGTAAGAGGT-3′	204	55
Cldn4	5′-TGTGGGCTACTGACTGCTTG-3′	5′-GTAACGTGGAGGCGAGAGAG-3′	325	50
Cldn8	5′-TATGACTCCCTGCTGGCTCT-3′	5′-AAGATGATTCCAGCCGTCAG-3′	179	50
Slc9a1	5′-GCAACTGGAGCAGAAGATCAC-3′	5′-CTGAGGCAGCGTTGTATTCTC-3′	369	55
Slc4a2	5′-AACTCTGGTGGAGGAGATGGT-3′	5′-CTGTCCTCTGCTTTGATCTGG-3′	657	55
Slc4a4	5′-ACTCCCTTCATTGCCTTTGTT-3′	5′-CGTCGCCAGATAGATGAAGAG-3′	552	55
Slc26a6	5′-TGTTCCTCGTCTGTGGAAGC-3′	5′-AGTCTACGCATGGCCTCATC-3′	933	51
Cftr	5′-TTATGACATTCACACCCAGCTC-3′	5′-TGTTAAGAATCCCACCTGCTTT-3′	609	55
Car2	5′-GAGCAACGGACCAGAGAACT-3′	5′-CCACCATGCTACCACCACAT-3′	950	51

bp, base pairs.

to block Na^+-H^+ exchange, 500μM H_2DIDS for Na^+-HCO_3^- cotransport, and 100μM acetazolamide for carbonic anhydrases. For stimulation of transport, 50μM ATP was used to elevate intracellular calcium, and 10μM forskolin, in combination with 500μM IBMX (3-isobutyl-1-methylxanthine), was used to elevate intracellular cAMP. All reagents were purchased from Sigma (Sigma-Aldrich), except H_2DIDS, BCECF-AM (Molecular Probes, Eugene, OR, USA), and cariporide (Santa Cruz Biotechnology).

Statistical analyses. Data are presented as the mean ± SEM. Statistical analyses were performed with 1-way or repeated measures analysis of variance, followed by Dunnett's post hoc test or an unpaired *t* test where only 2 groups had to be compared. In the transepithelial resistance experiments, large differences in SEM did not permit the application of parametric tests. In this case, the nonparametric Kruskal-Wallis test and Dunn's post hoc test were used to compare values.

Buffering Capacity of Hat-7 Cells

The buffering capacity of HAT-7 cells was measured to convert rates of pH change to equivalent base fluxes as described previously (Szucs et al. 2006). pH_i is slightly variable depending on the metabolic state of the cells and actual and predisposing conditions, such as minor changes in pH of the medium, temperature, moving Transwells from cell incubator to the experimental setup, and so on. To exclude the errors introduced by pH change (which is actually a logarithmic scale), we always calculate the flux (i.e., the quantity of ions). This becomes very important in the case of large pH changes, as in during an acid load or a base load. As an example, the decrease of pH from 7 to 6.9 means 10 times more proton movement than a pH change from 8 to 7.9. Buffering capacity is by definition the amount of acid/base that changes pH by 1 unit. Total buffering capacity (β_t) consists of an intrinsic component (β_i, the buffering capacity of proteins and other cellular components) and the buffering capacity of the HCO_3^-/CO_2 buffer system (β_{co2}). Both components vary with pH_i. The first component can be measured in HCO_3^-/CO_2-free conditions (i.e., in a HEPES-buffered solution) by the stepwise addition of NH_4^+, while cellular pH compensatory mechanisms are blocked by continuous extracellular Na^+ withdrawal (Appendix Fig. A). The latter component can be calculated according to the Henderson-Hasselbalch equation per the partial pressure and solubility of CO_2 at 37 °C. Total buffering capacity was determined as a function of pH_i by adding the predicted contribution of the HCO_3^-/CO_2 buffer system. Total and intrinsic buffering capacity values plotted against pH_i are shown in Appendix Figure B. A trend line was fitted by nonlinear regression to the total buffering capacity data and was used to calculate the buffering capacity values for the subsequent functional measurements. Our data indicate that, within the pH_i range at which these measurements were made (6.5 to 7.5), the intracellular buffering capacity of HAT-7 cells was approximately 40 mM. Apparent base fluxes were calculated by multiplying the rate of change of pH_i by the total buffering capacity at the corresponding pH_i value.

Appendix Table 2. Predesigned Real-time Primers.

Cldn1	Rn00581740_m1
Cldn4	Rn01196224_s1
Cldn8	Rn01767199_s1
Tjp1	Rn02116071_s1
Slc9a1	Rn00561924_m1
Slc4a2	Rn00566910_m1
Slc4a4	Rn00584747_m1
Slc26a4	Rn00693043_m1
Cftr	Rn01455971_m1
Car2	Rn01462065_m1
Klk4	Rn01498536_m1
Rplp0	Rn00821065_g1

Appendix References

Bronckers AL, Guo J, Zandieh-Doulabi B, Bervoets TJ, Lyaruu DM, Li X, Wangemann P, DenBesten P. 2011. Developmental expression of solute carrier family 26A member 4 (SLC26A4/pendrin) during amelogenesis in developing rodent teeth. Eur J Oral Sci. 119 Suppl 1:185–192.

Bronckers AL, Lyaruu DM, Jansen ID, Medina JF, Kellokumpu S, Hoeben KA, Gawenis LR, Oude-Elferink RP, Everts V. 2009. Localization and function of the anion exchanger Ae2 in developing teeth and orofacial bone in rodents. J Exp Zool B Mol Dev Evol. 312B(4):375–387.

Jalali R, Guo J, Zandieh-Doulabi B, Bervoets TJ, Paine ML, Boron WF, Parker MD, Bijvelds MJ, Medina JF, DenBesten PK, et al. 2014. NBCe1

(SLC4A4) a potential pH regulator in enamel organ cells during enamel development in the mouse. Cell Tissue Res. 358(2):433–442.

Jalali R, Zandieh-Doulabi B, DenBesten PK, Seidler U, Riederer B, Wedenoja S, Micha D, Bronckers AL. 2015. Slc26a3/Dra and Slc26a6 in murine ameloblasts. J Dent Res. 94(12):1732–1739.

Reibring CG, El Shahawy M, Hallberg K, Kannius-Janson M, Nilsson J, Parkkila S, Sly WS, Waheed A, Linde A, Gritli-Linde A. 2014. Expression patterns and subcellular localization of carbonic anhydrases are developmentally regulated during tooth formation. PLoS One. 9(5):e96007.

Szlavik V, Szabo B, Vicsek T, Barabas J, Bogdan S, Gresz V, Varga G, O'Connell B, Vag J. 2008. Differentiation of primary human submandibular gland cells cultured on basement membrane extract. Tissue Eng Part A. 14(11):1915–1926.

Szucs A, Demeter I, Burghardt B, Ovari G, Case RM, Steward MC, Varga G. 2006. Vectorial bicarbonate transport by Capan-1 cells: a model for human pancreatic ductal secretion. Cell Physiol Biochem. 18(4–5):253–264.

Thomas JA, Buchsbaum RN, Zimniak A, Racker E. 1979. Intracellular pH measurements in Ehrlich ascites tumor cells utilizing spectroscopic probes generated in situ. Biochemistry. 18(11):2210–2218.